Modeling Dusty Star Forming Galaxies and High-z Massive Quiescents

Pablo Araya-Araya
Postdoc at DTU-Space/DAWN

HST Image: NGC1376

HST Image: ESO325

HST Image: Arp244

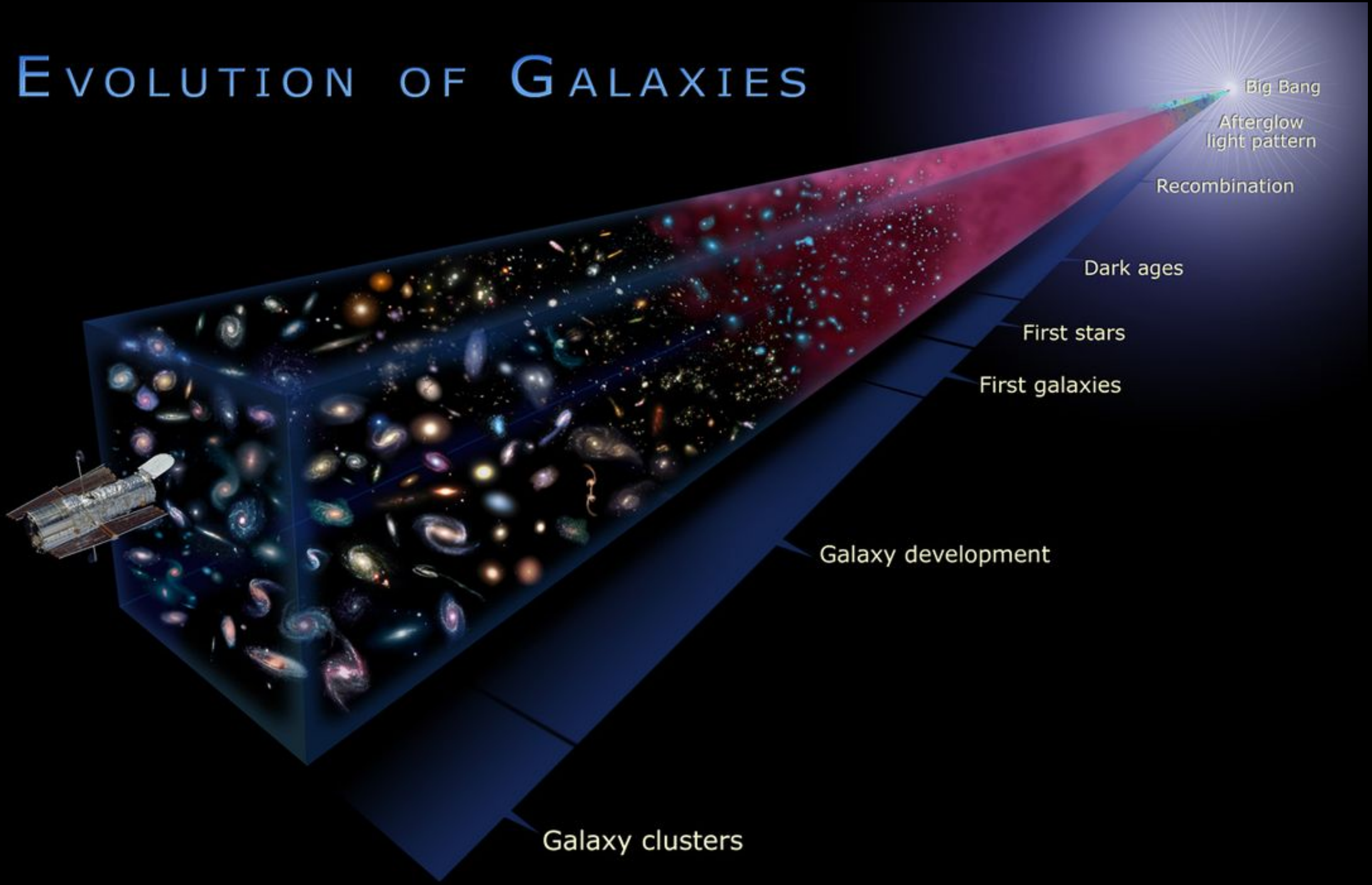

Credits: NASA, ESA, and A. Feild (STScI)

Testing our understanding about galaxy formation and evolution: Simulations

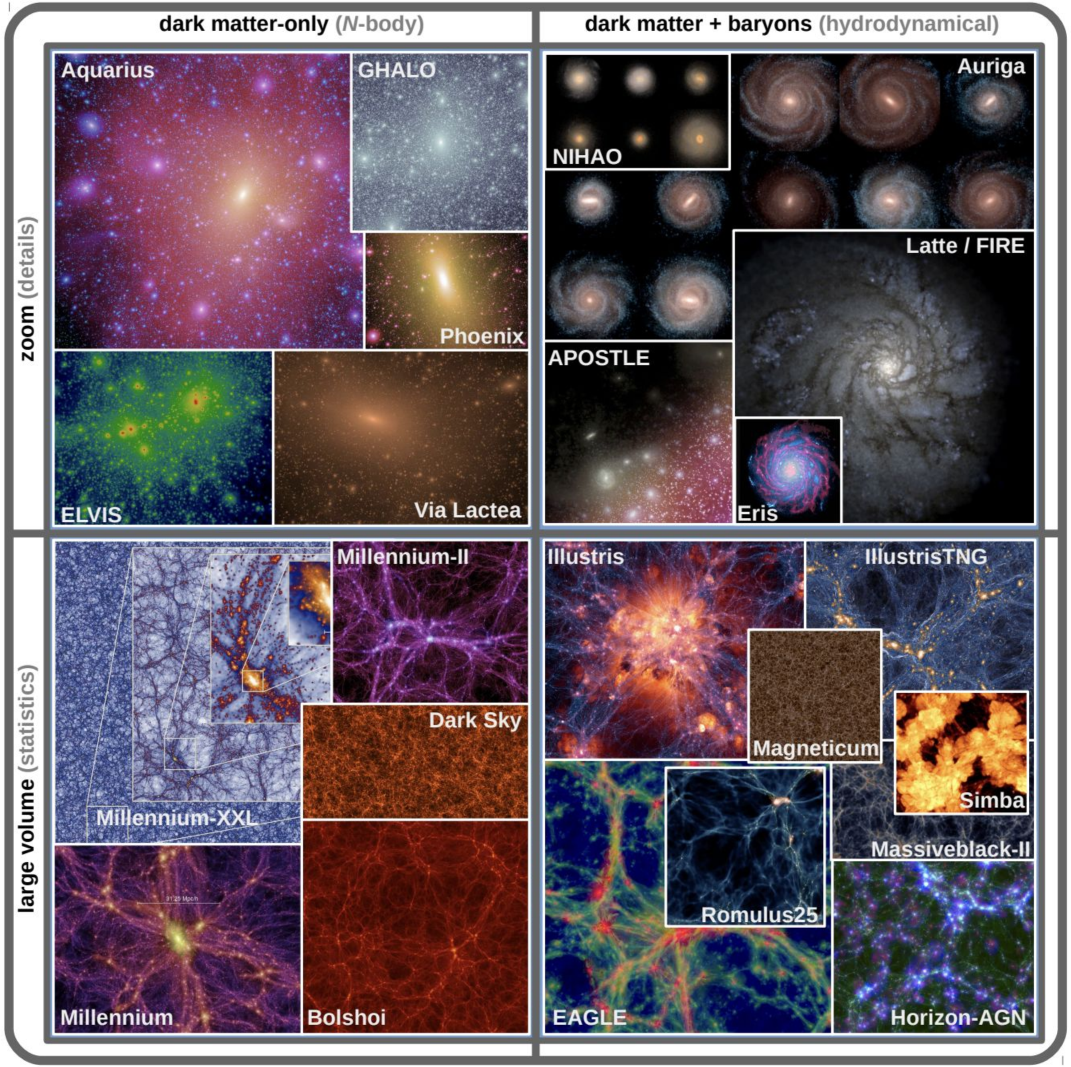

Vogelsberger+20

Testing our understanding about galaxy formation and evolution: Simulations

Dark matter only simulations:
large volumes → more rare systems

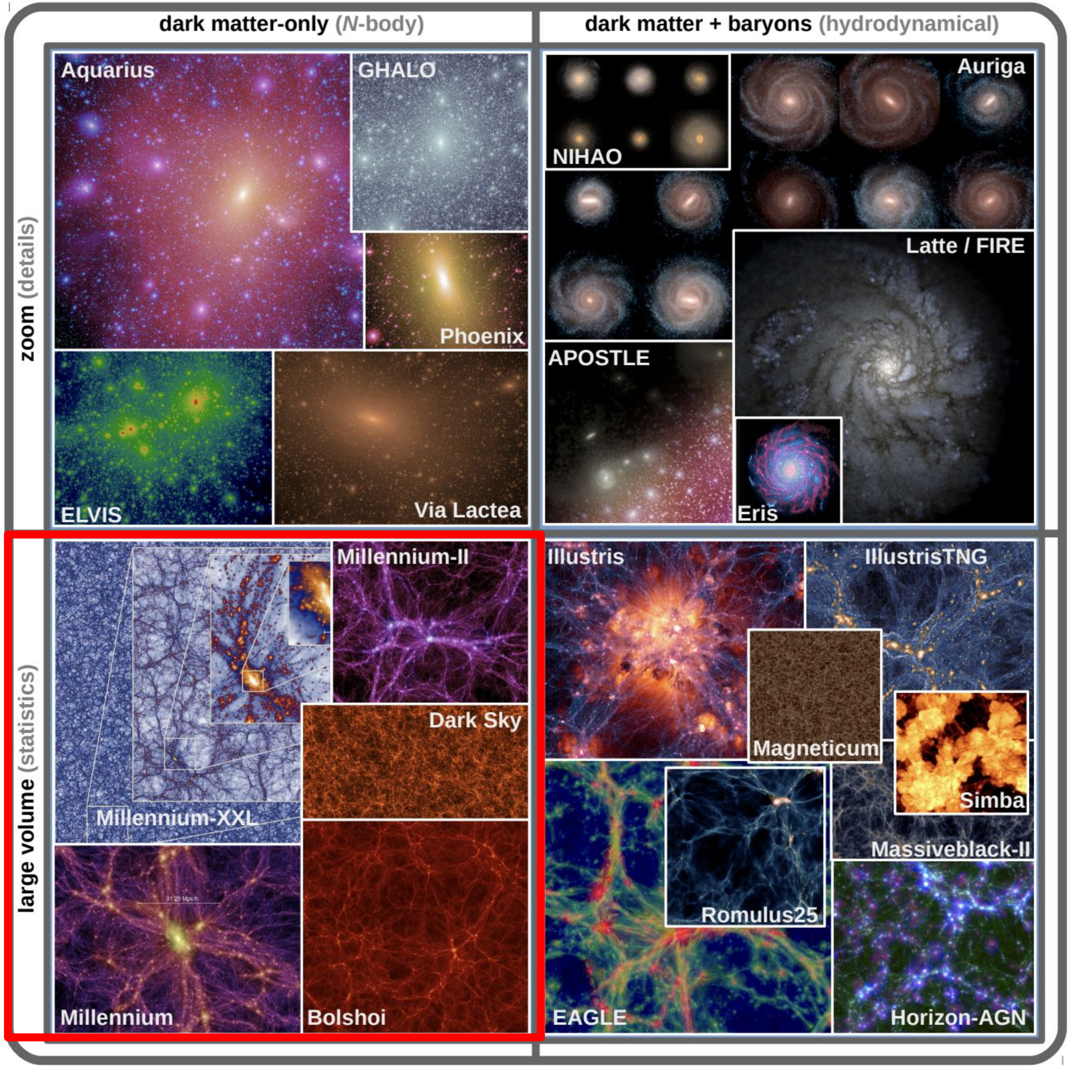

Vogelsberger+20

Semi-analytical models (SAMs)

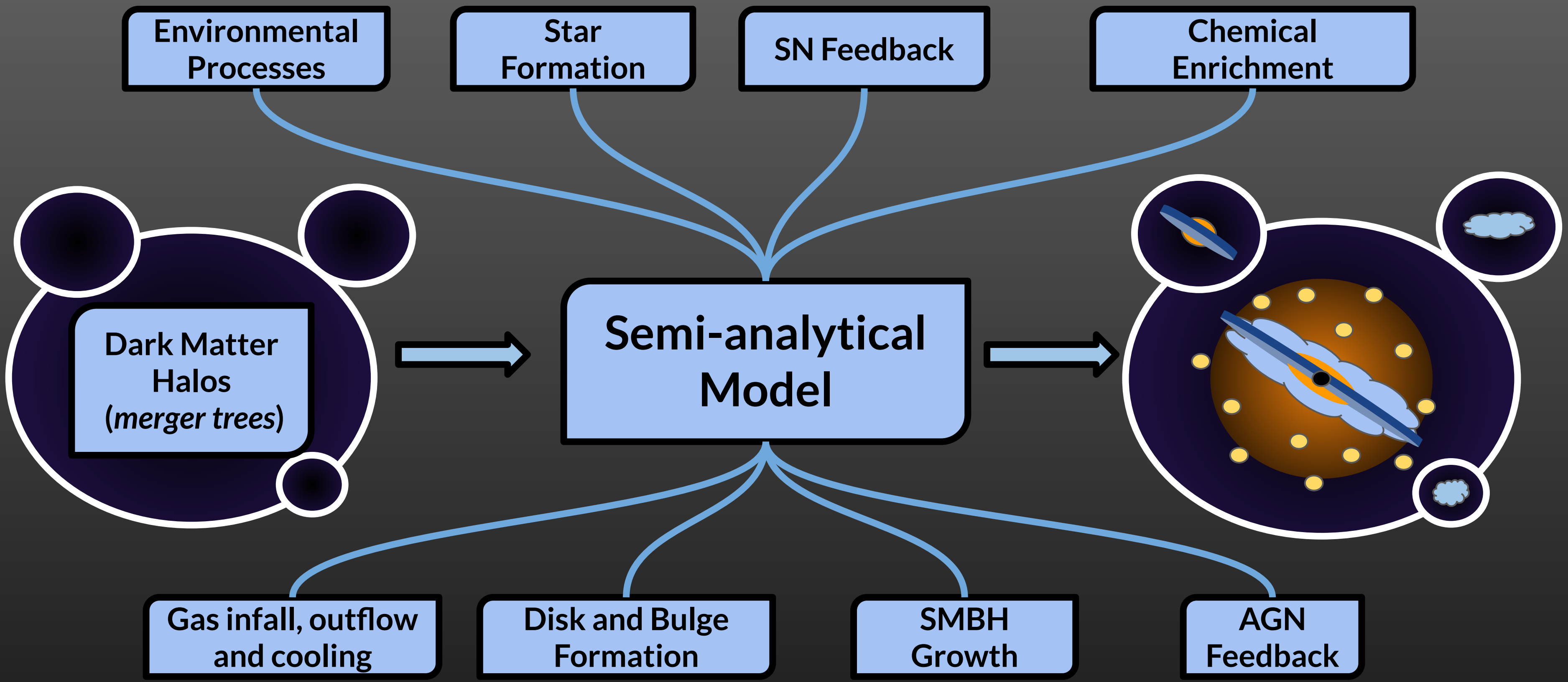

Long-standing tension:

Dusty Star Forming Galaxies: Massive galaxies with bright IR luminosities (dust emission), detected at the sub-mm.

See Miranda Andersen talk for more about DSFGs!

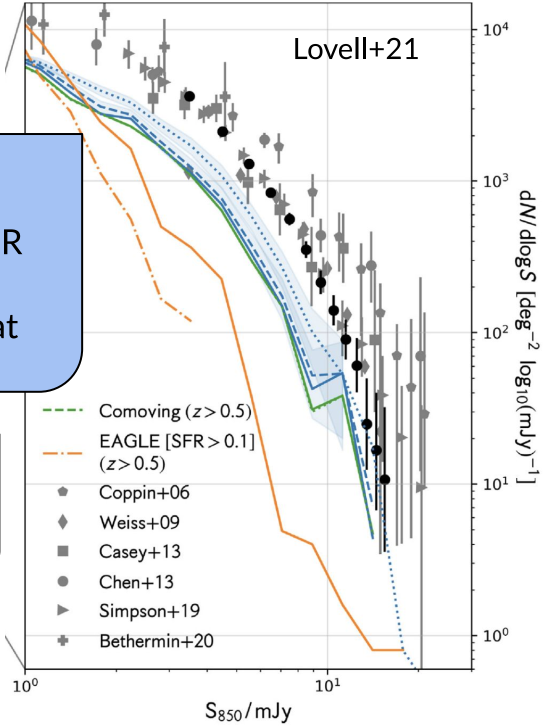

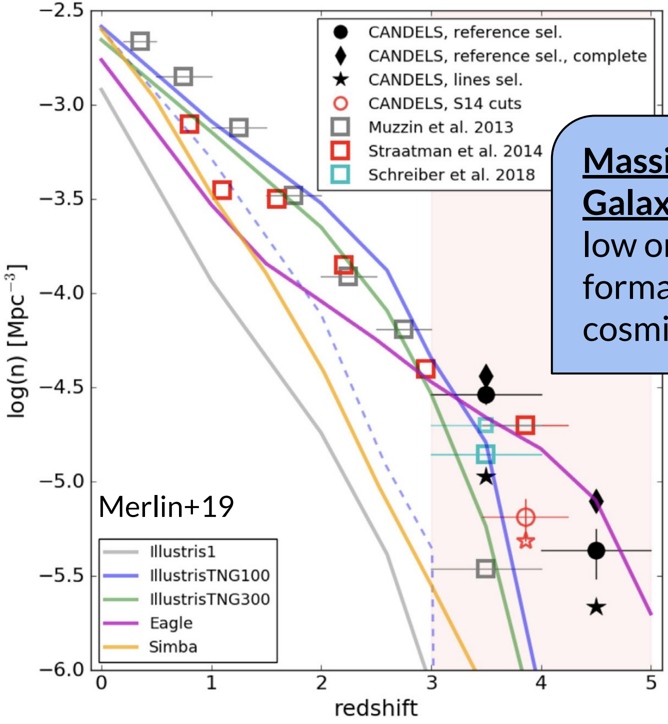

Massive Quiescent Galaxies: Galaxies with low or null star formation rates at the cosmic noon.

Models that match the sub-mm number counts critically underpredict the abundance of quiescent galaxies at high-z, and viceversa.

Semi-analytical models (SAMs)

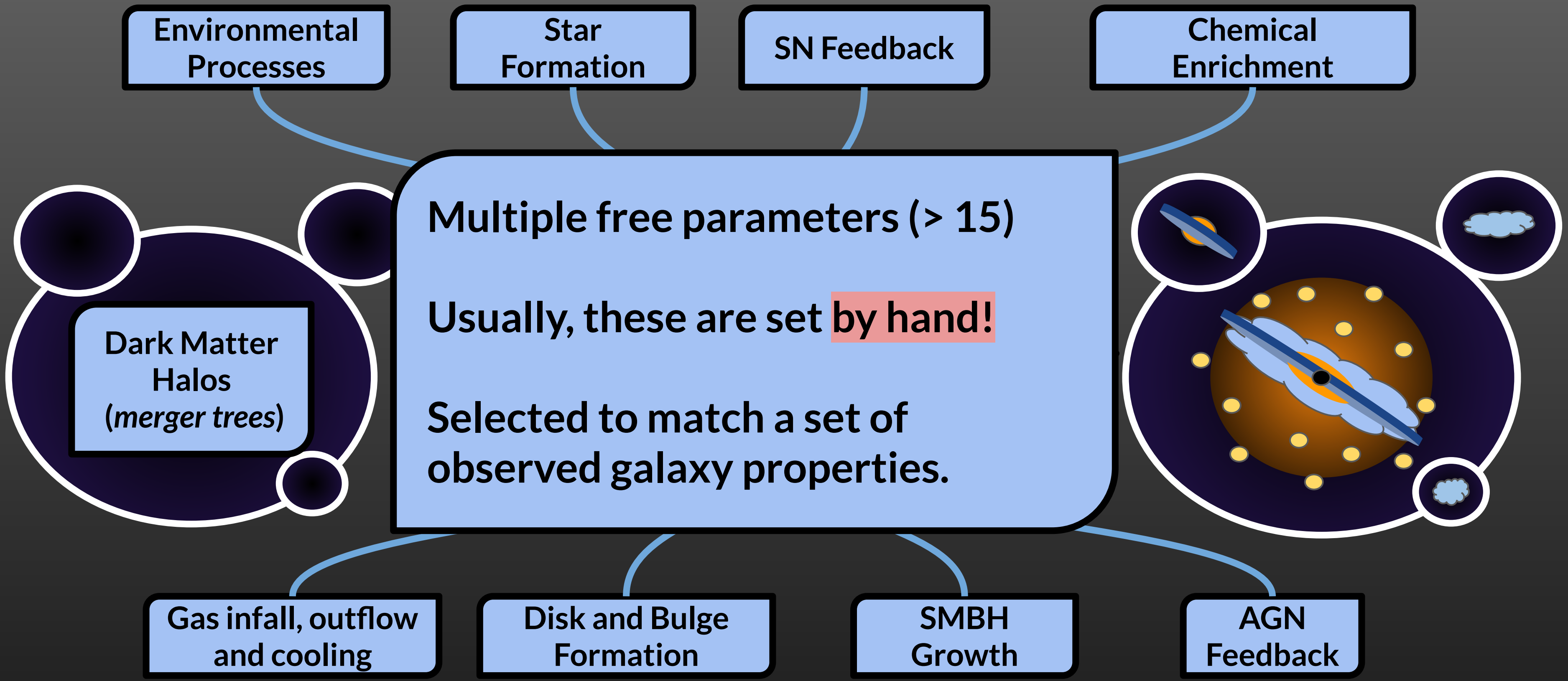

Recalibrating L-Galaxies, the MCMC-mode

◆ Henriques+20 version of L-Galaxies SAM.

◆ Representative sample of merger trees.

◆ Set of observational constraints:

◆ Similar to H20, but SMFs and f_Q from Leja+20;+21

◆ Include the number density of SMGs (AS2UDS survey; Dudzevičiūtė+20)

◆ **Patience**. We used 1M of CPU hours (~7000 x 96; steps x chains)

Sets of observational constraints

Table 1. List of MCMC configurations used throughout this paper.

Config	SMF $z = 0.4$	SMF $z = 2.8$	f_Q $z = 0.4$	f_Q $z = 2.8$	n_{SMG} $z = 2.8$	HIMF $z = 0$
0: base_{H20}	✓	✓	✓	✓		✓
1: base_{L20}	✓	✓	✓	✓		✓
2: all($\mathrm{base}_{L20}+n_{SMG}$)	✓	✓	✓	✓	✓	✓
3: no hi-z SMF	✓		✓	✓	✓	✓
4: no hi-z f_Q	✓	✓	✓		✓	✓
5: no hi-z SMF, f_Q	✓		✓		✓	✓
6: no HI MF	✓	✓	✓	✓	✓	
7: no low-z f_Q	✓	✓		✓	✓	✓
8: no low-z SMF, f_Q		✓		✓	✓	✓

The predicted sub-mm number counts

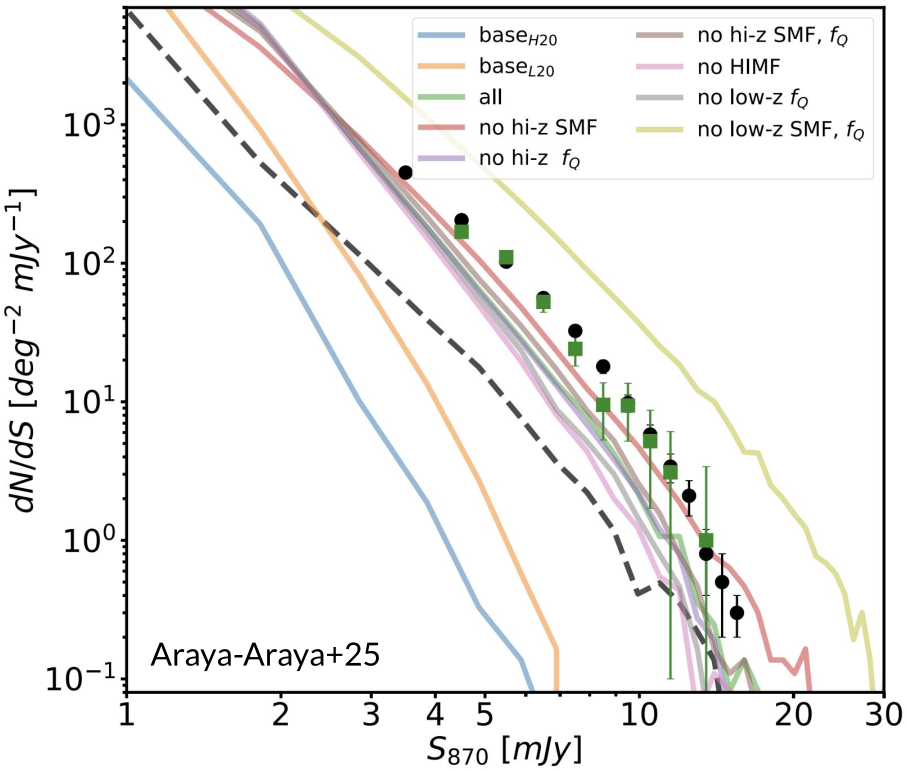

Config	SMF $z = 0.4$	SMF $z = 2.8$	f_Q $z = 0.4$	f_Q $z = 2.8$	n_{SMG} $z = 2.8$	HIMF $z = 0$
0: base$_{H20}$	✓	✓	✓	✓		✓
1: base$_{L20}$	✓	✓	✓	✓		✓
2: all(base$_{L20}$+n_{SMG})	✓	✓	✓	✓	✓	✓
3: no hi-z SMF	✓		✓	✓	✓	✓
4: no hi-z f_Q	✓	✓	✓		✓	✓
5: no hi-z SMF, f_Q	✓		✓		✓	✓
6: no HI MF	✓	✓	✓	✓	✓	
7: no low-z f_Q	✓	✓		✓	✓	✓
8: no low-z SMF, f_Q		✓		✓	✓	✓

The predicted sub-mm number counts

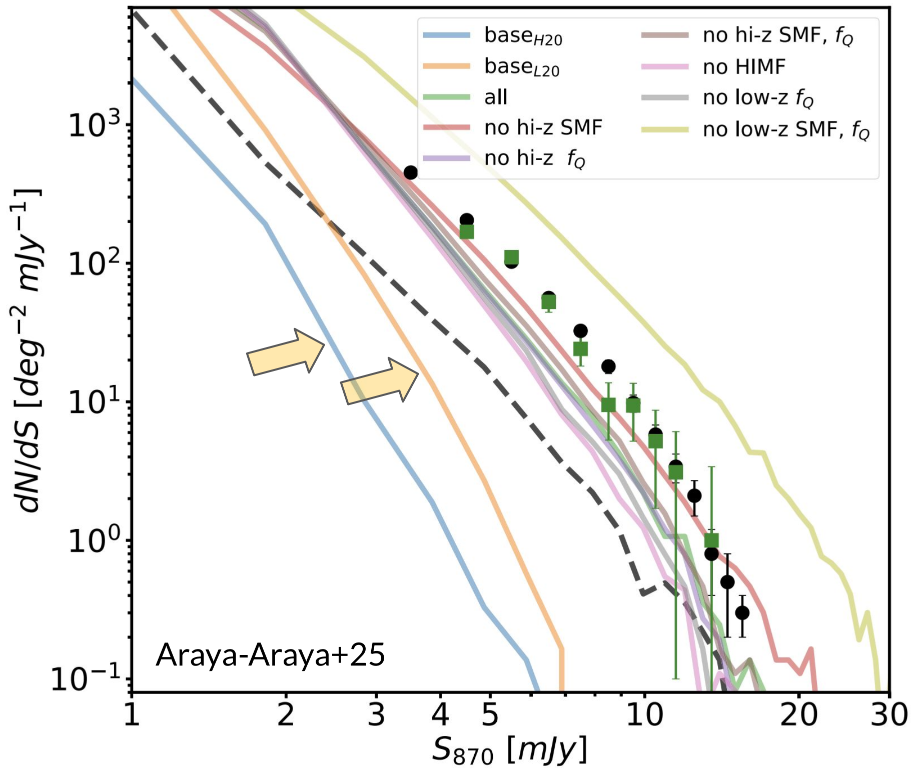

Config	SMF $z = 0.4$	SMF $z = 2.8$	f_Q $z = 0.4$	f_Q $z = 2.8$	n_{SMG} $z = 2.8$	HIMF $z = 0$
0: base$_{H20}$	✓	✓	✓	✓		✓
1: base$_{L20}$	✓	✓	✓	✓		✓
2: all(base$_{L20}$+n_{SMG})	✓	✓	✓	✓	✓	✓
3: no hi-z SMF	✓		✓	✓	✓	✓
4: no hi-z f_Q	✓	✓	✓		✓	✓
5: no hi-z SMF, f_Q	✓		✓		✓	✓
6: no HI MF	✓	✓	✓	✓	✓	
7: no low-z f_Q	✓	✓		✓	✓	✓
8: no low-z SMF, f_Q		✓		✓	✓	✓

The models critically underpredict the sub-mm number counts when n_{SMG} is not used.

The predicted sub-mm number counts

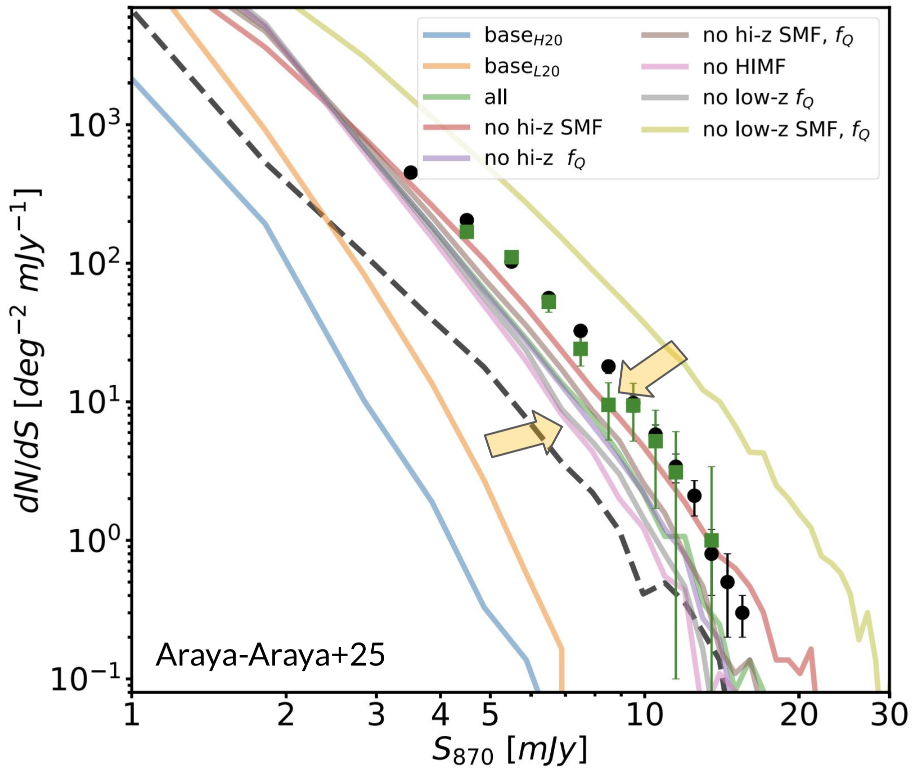

Config	SMF $z = 0.4$	SMF $z = 2.8$	f_Q $z = 0.4$	f_Q $z = 2.8$	n_{SMG} $z = 2.8$	HIMF $z = 0$
0: base$_{H20}$	✓	✓	✓	✓		✓
1: base$_{L20}$	✓	✓	✓	✓		✓
2: all(base$_{L20}$+n_{SMG})	✓	✓	✓	✓	✓	✓
3: no hi-z SMF	✓		✓	✓	✓	✓
4: no hi-z f_Q	✓	✓	✓		✓	✓
5: no hi-z SMF, f_Q	✓		✓		✓	✓
6: no HI MF	✓	✓	✓	✓	✓	
7: no low-z f_Q	✓	✓		✓	✓	✓
8: no low-z SMF, f_Q		✓		✓	✓	✓

The models critically underpredict the sub-mm number counts when n_{SMG} is not used.

Most of our models closely match the observed sub-mm number counts!

Reproducing the DSFGs population, physical aspects

SN feedback: efficiency in (re)heating cold gas (suppressing cooling)

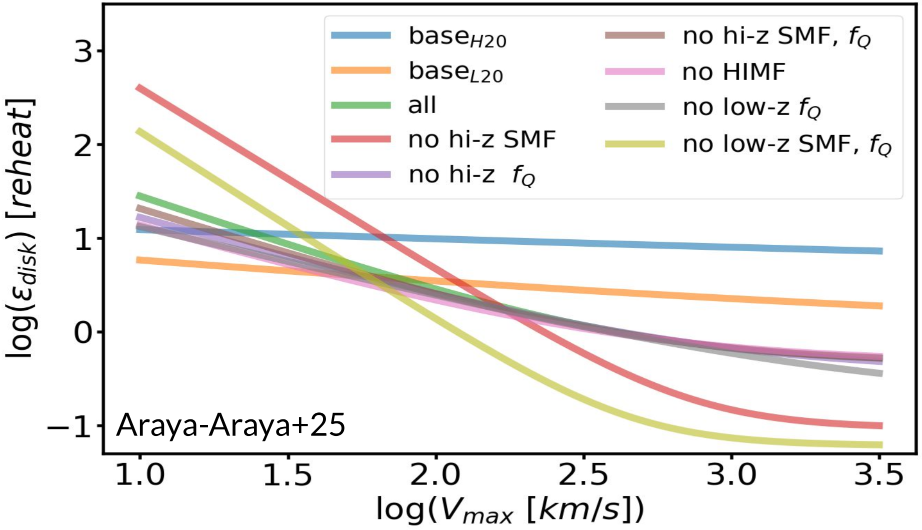

$$\epsilon_x = \eta_x \times \left[0.5 + \left(\frac{V_{\rm max}}{V_x}\right)^{-\beta_x}\right]$$

η_x, V_x, and α_x free parameters

Secular star formation rate efficiency (Kennicutt-Schmidt relation)

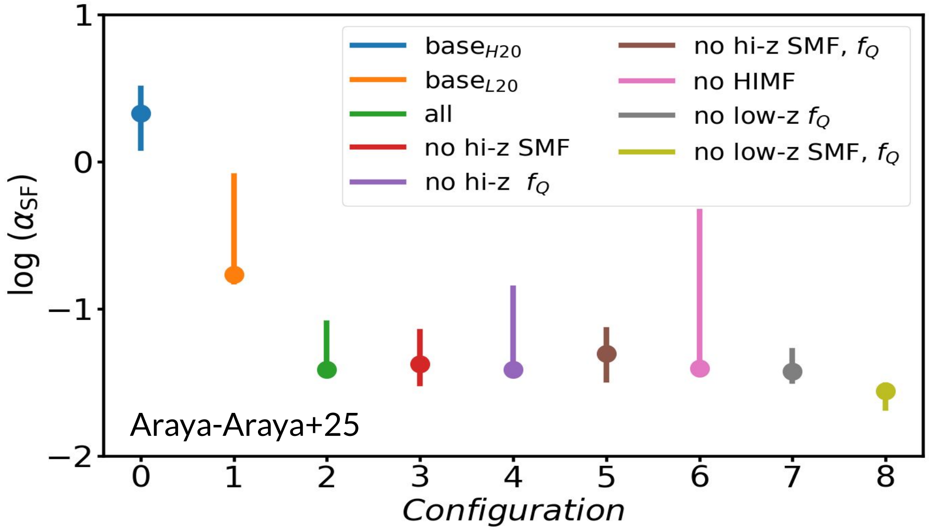

Reproducing the DSFGs population, physical aspects

SN feedback: efficiency in (re)heating cold gas (suppressing cooling)

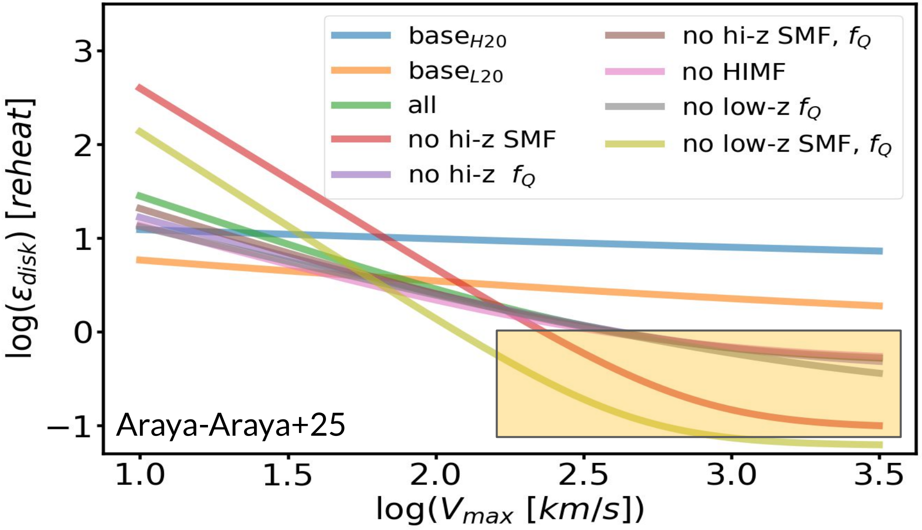

$$\epsilon_x = \eta_x \times \left[0.5 + \left(\frac{V_{\max}}{V_x}\right)^{-\beta_x}\right]$$

η_x, V_x, and α_x free parameters

Secular star formation rate efficiency (Kennicutt-Schmidt relation)

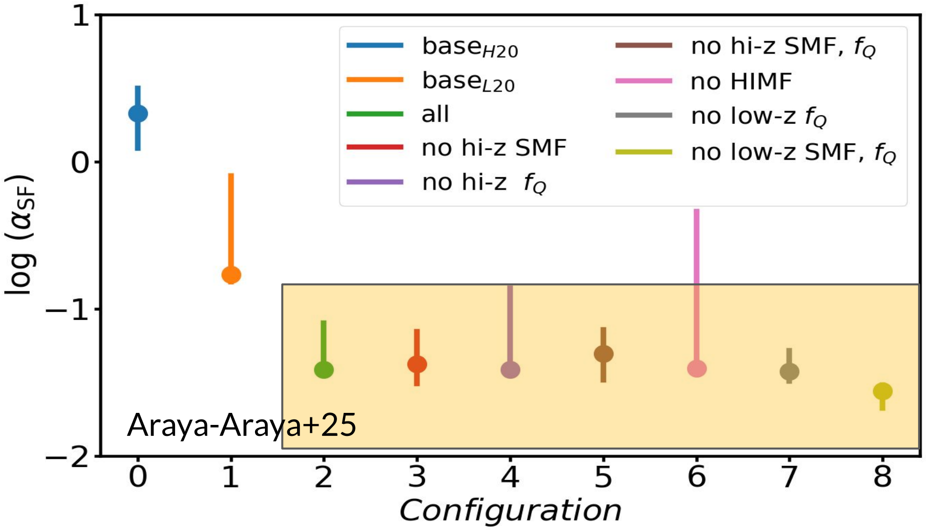

The predicted number density of high-z massive quiescents

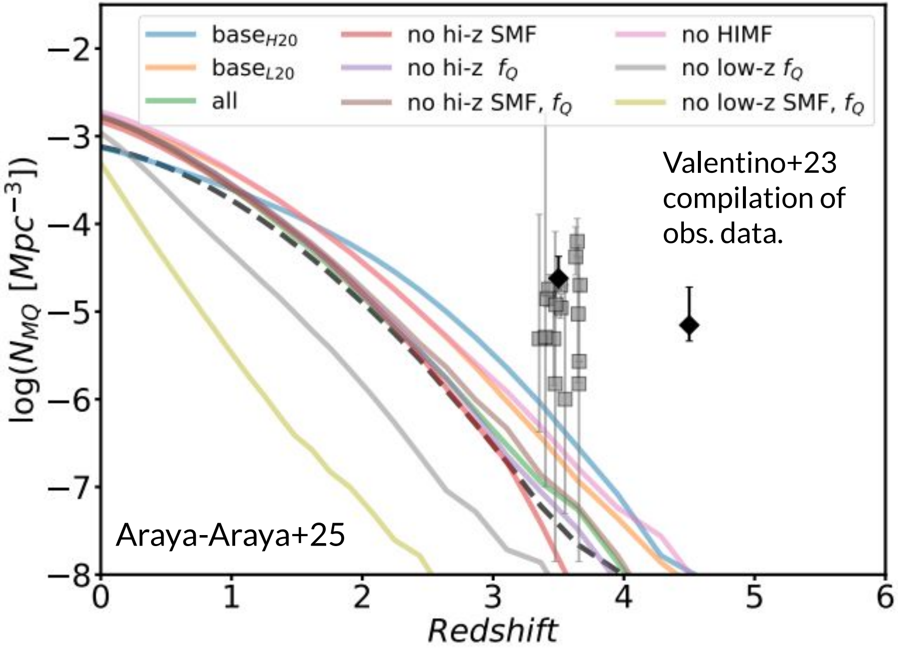

Massive Quiescents (MQs):

$\log(M_\star/M_\odot) > 10.6$

sSFR/yr < 0.2/t(z)

The predicted number density of high-z massive quiescents

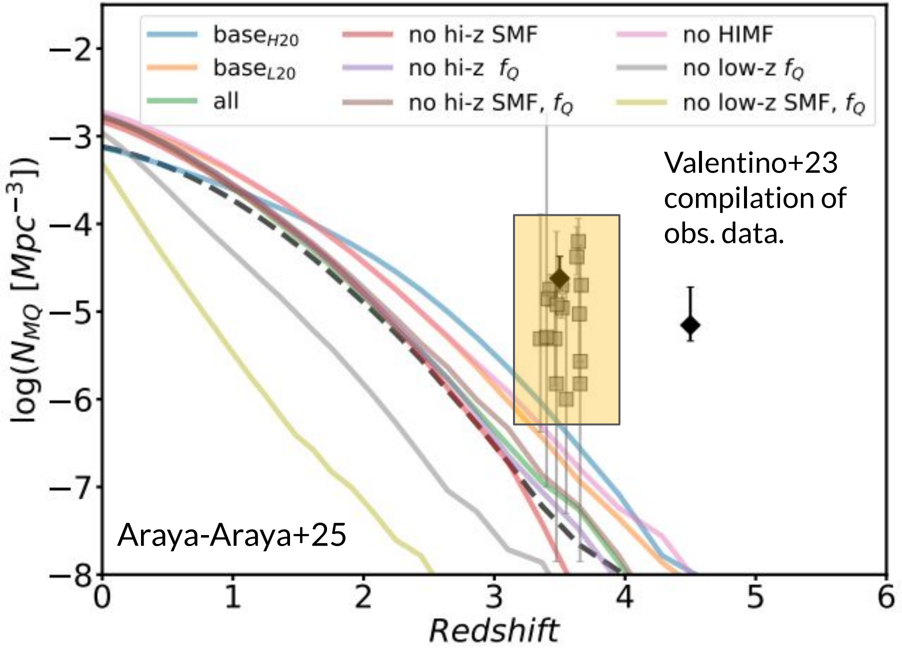

Massive Quiescents (MQs):
$\log(M_\star / M_\odot) > 10.6$
sSFR/yr < 0.2/t(z)

Observations are highly uncertain!

The predicted number density of high-z massive quiescents

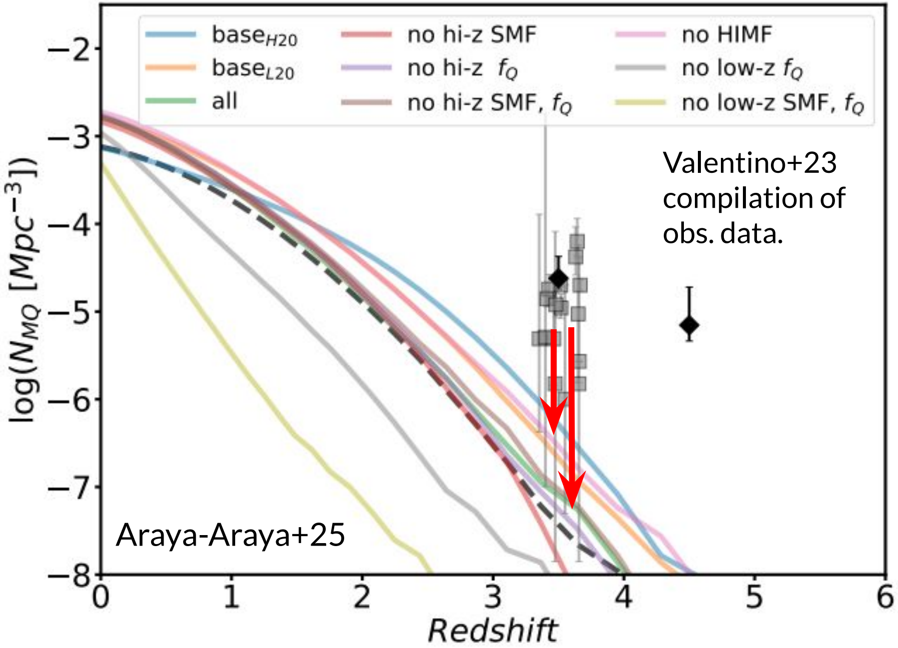

Massive Quiescents (MQs):
$\log(M_\star/M_\odot) > 10.6$
sSFR/yr < 0.2/t(z)

Observations are highly uncertain!

Most of our models critically underpredict the abundance of z ~ 3.5 MQs.

The predicted number density of high-z massive quiescents

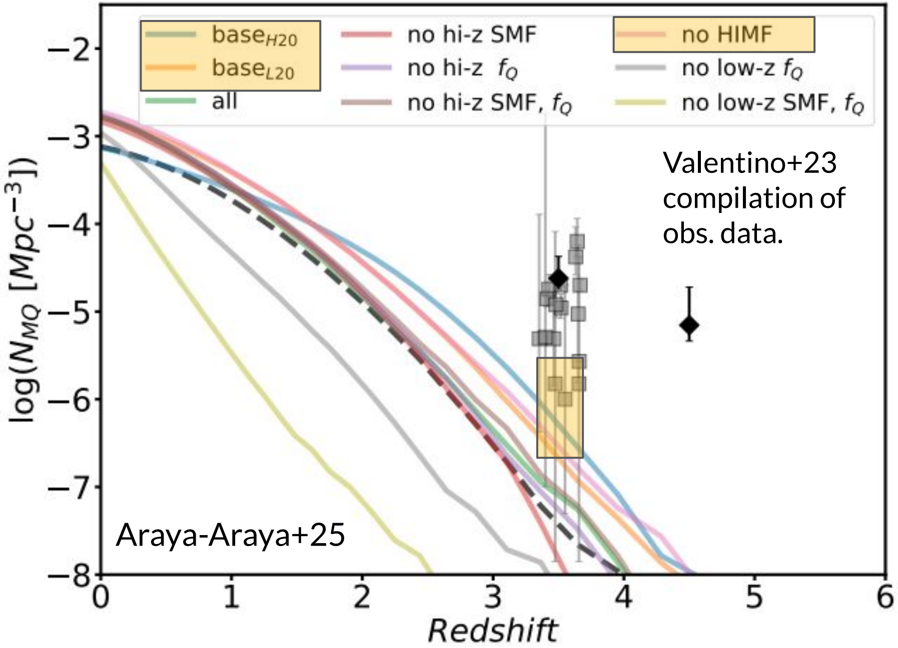

Massive Quiescents (MQs):
$\log(M_\star / M_\odot) > 10.6$
sSFR/yr < 0.2/t(z)

Observations are highly uncertain!

Most of our models critically underpredict the abundance of z ~ 3.5 MQs.

Three of our models are consistent only with the observed lower limits.

Simultaneously modeling DSFGs and MQs at high-z

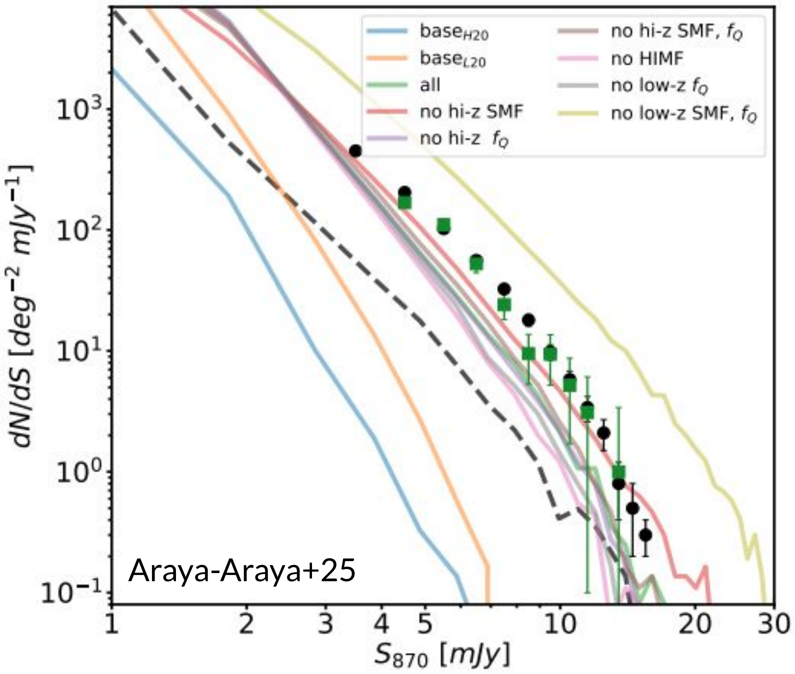

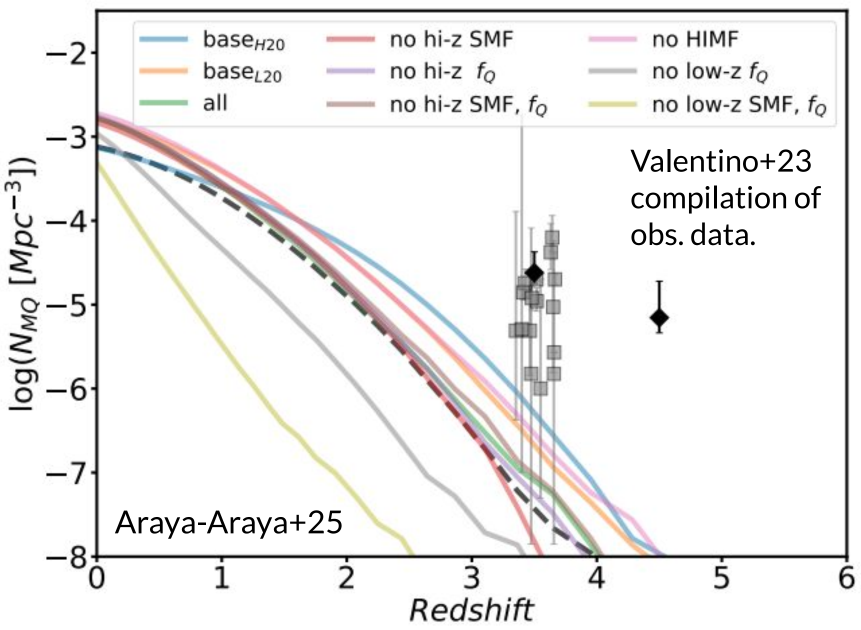

Valentino+23 compilation of obs. data.

Simultaneously modeling DSFGs and MQs at high-z

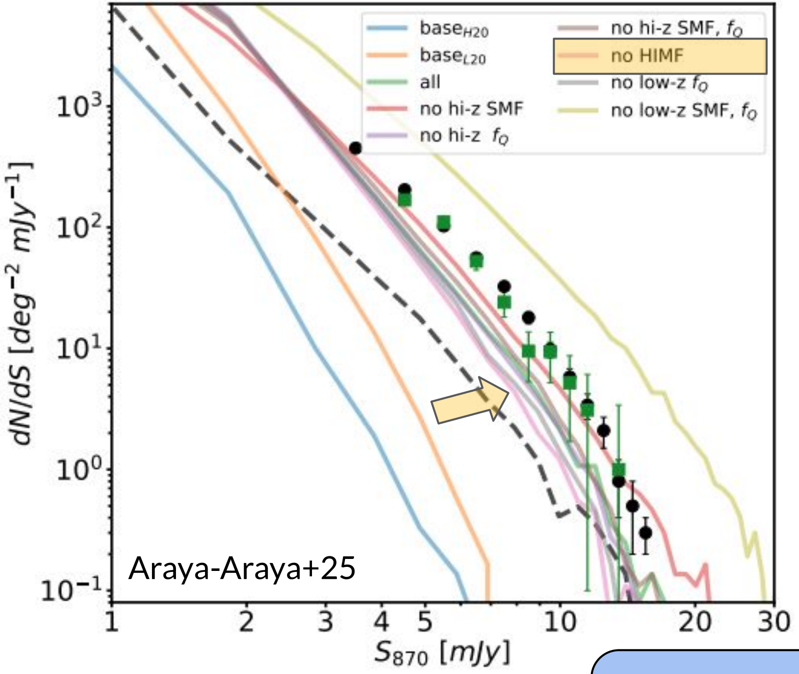

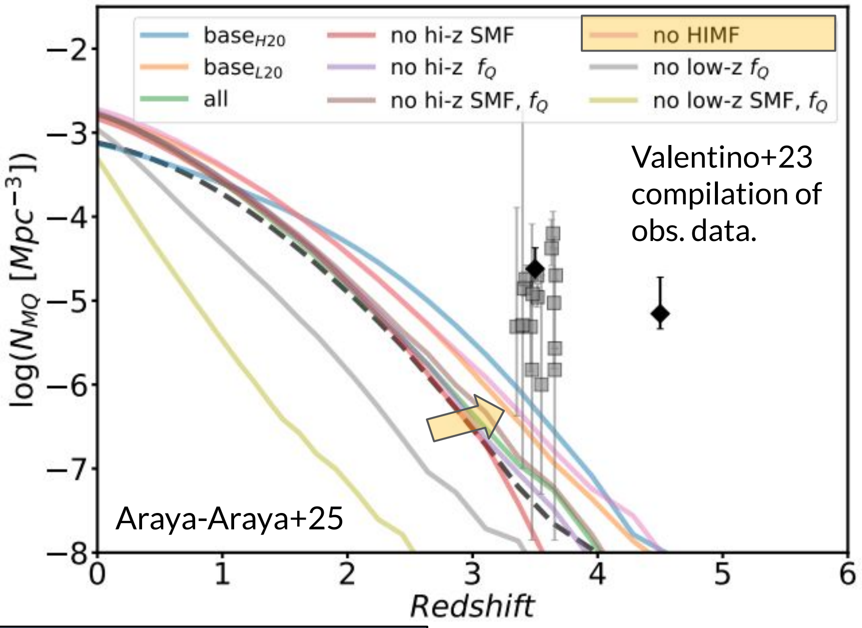

The configuration "no HIMF" is "in between" the tension!

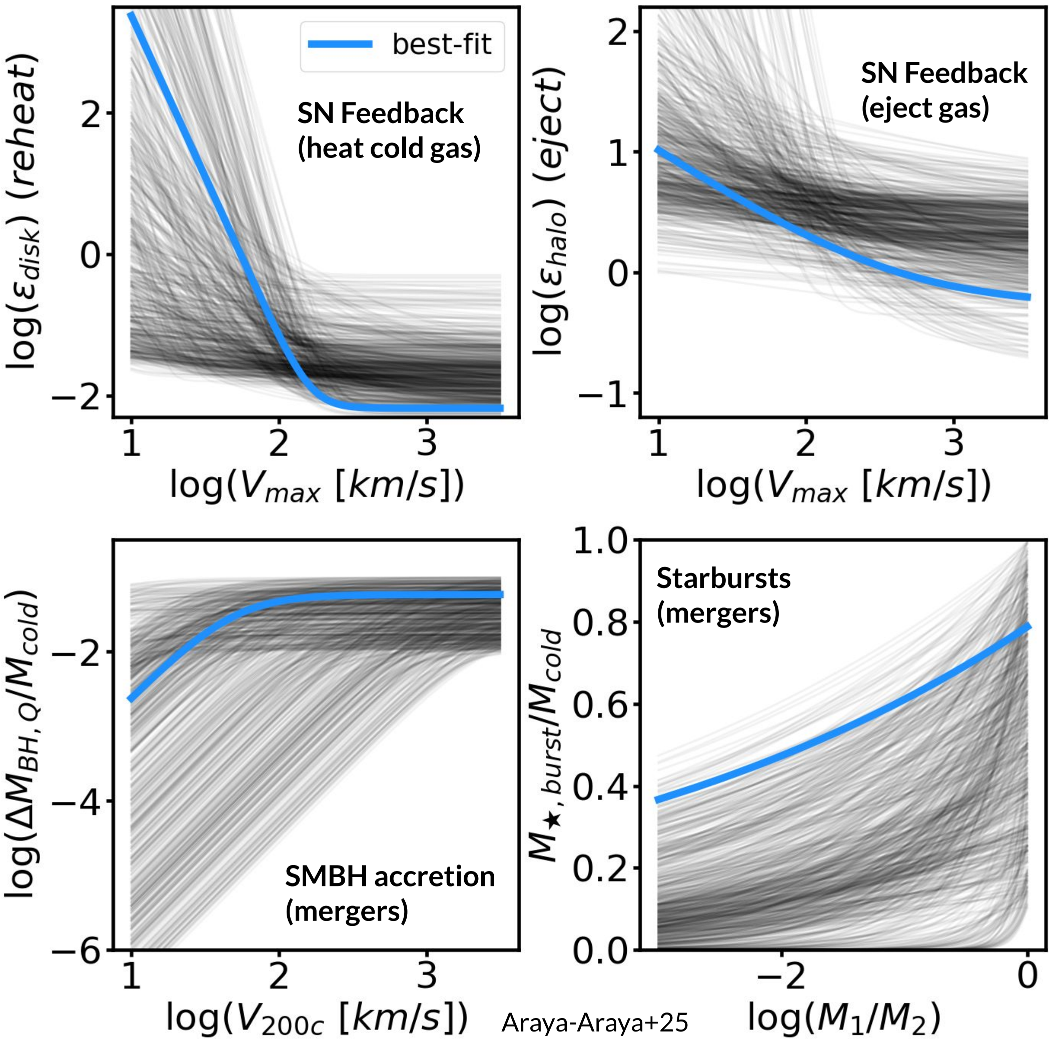

Araya-Araya+25

Highly degenerated space

Models with similar likelihoods (within 1 dex of best-fit) yield different underlying physics.

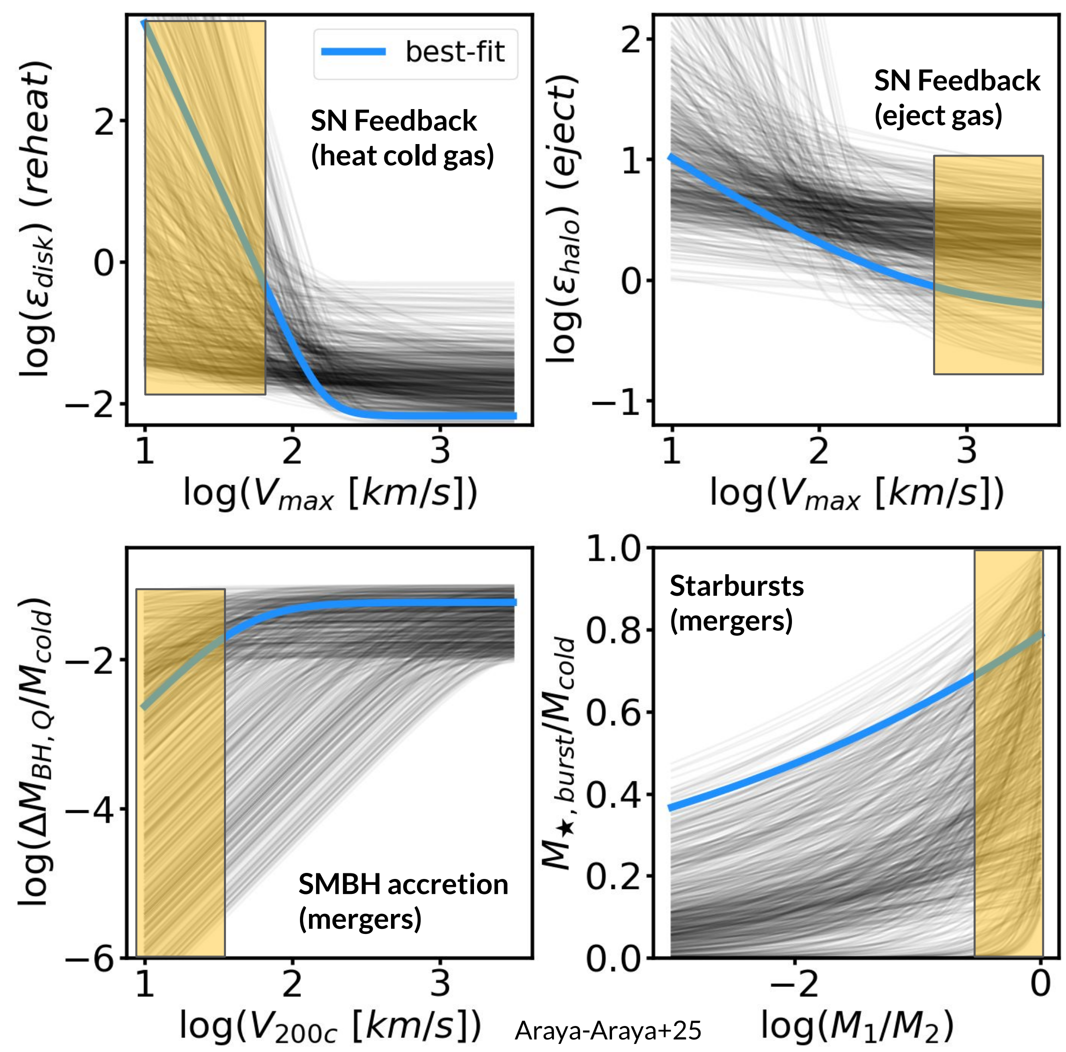

Highly degenerated space

Models with similar likelihoods (within 1 dex of best-fit) yield different underlying physics.

A systematic exploration of the galaxy formation hyperdimensional space is needed!

Summary

◆ All the models calibrated by using the number density of SMGs closely matched the sub-mm number counts.

◆ However, all our recalibrated models struggle to recover the abundance of high-z massive quiescent galaxies.
The tension persists.

◆ One configuration, “no HIMF”, reasonably reproduces both observables.

◆ The hyperdimensional space of L-Galaxies (and galaxy formation models) is highly degenerated, highlighting the importance of systematic and robust calibration methods.

*Comparison with other observables in Araya-Araya+25

*DSFGs and high-z MQs are connected, check Araya-Araya+26

Pablo Araya Araya
e-mail: paaar@dtu.dk

The simulation and sub-mm emission model

Cochrane+23 scaling relations:
FIRE zoom-in simulation (Hopkins+14,18)
+ SKIRT radiative transfer code
(Baes+11,15):

◆ Link global galaxy properties with sub-mm flux densities derived from SKIRT

$$S_\nu/\mathrm{mJy} = \alpha \left(\frac{\mathrm{SFR}_{10}}{100\,\mathrm{M}_\odot \mathrm{yr}^{-1}} \right)^{\beta} \left(\frac{\mathrm{M}_\star}{10^{10}\,\mathrm{M}_\odot} \right)^{\gamma} \left(\frac{\mathrm{M}_{\mathrm{dust}}}{10^{8}\,\mathrm{M}_\odot} \right)^{\delta} (1+z)^{\eta}. \quad (2)$$

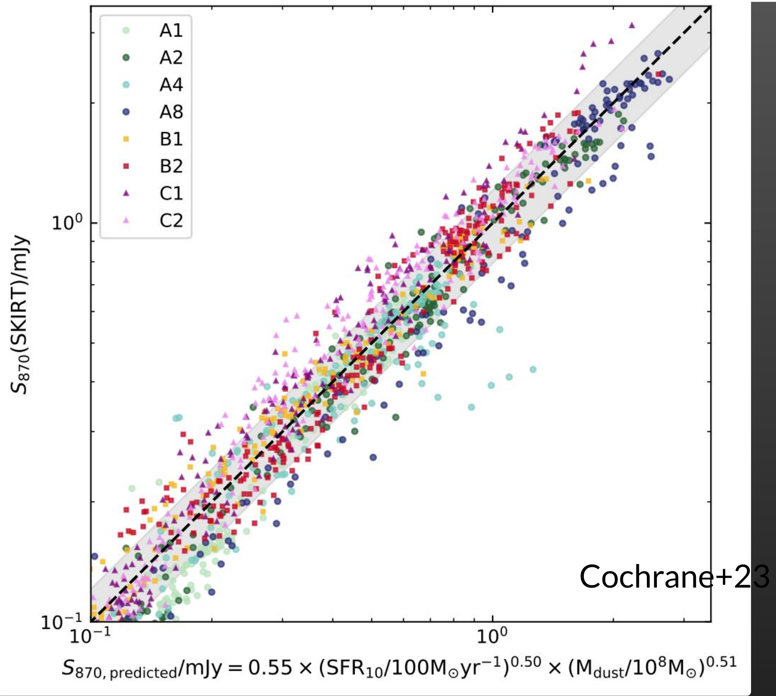

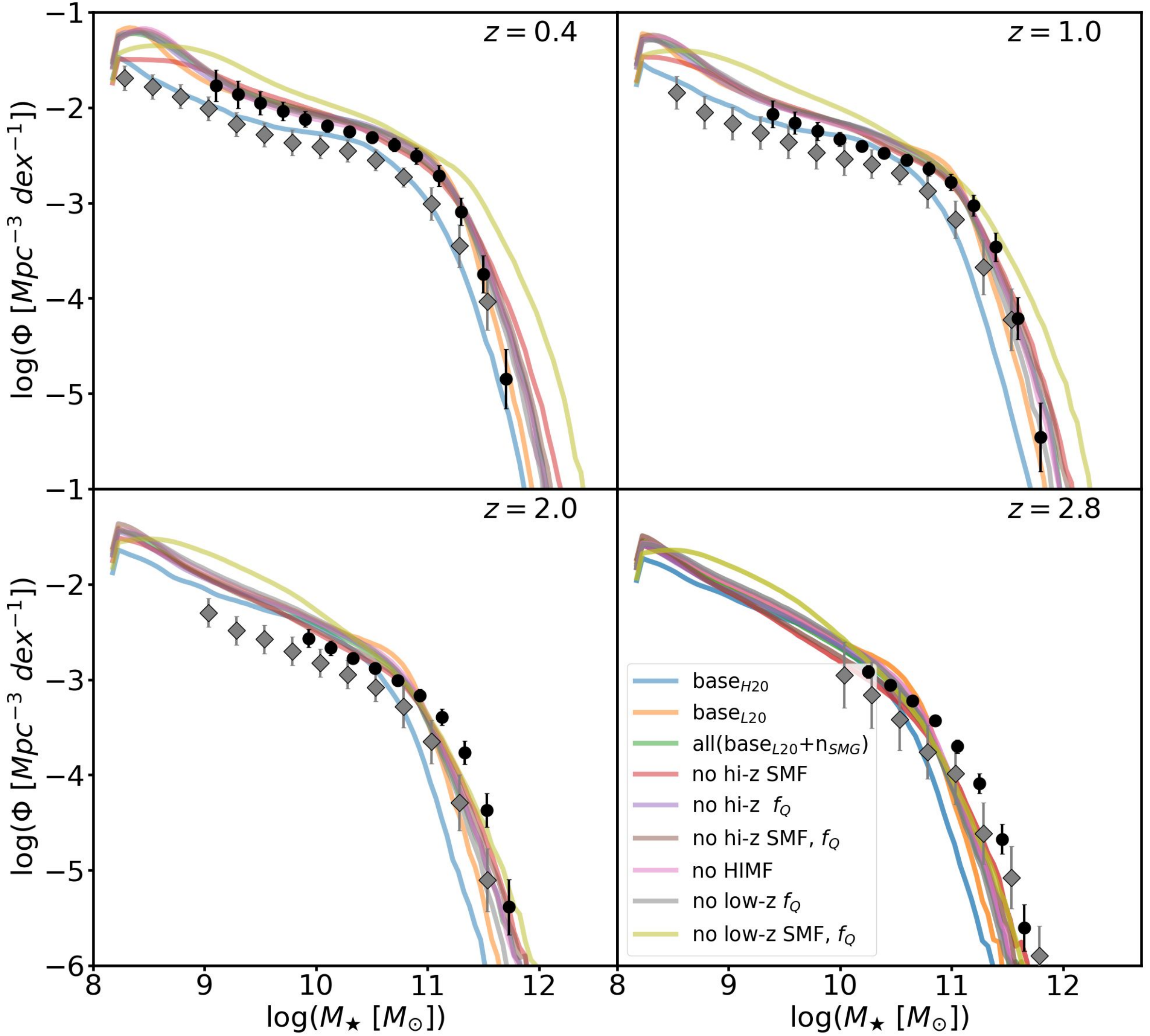

Stellar Mass Functions

- Reasonable agreement at $z \lesssim 2$
- Struggle at the massive end at high redshift, regardless of SMF used for calibration

Fraction of Quiescent Galaxies

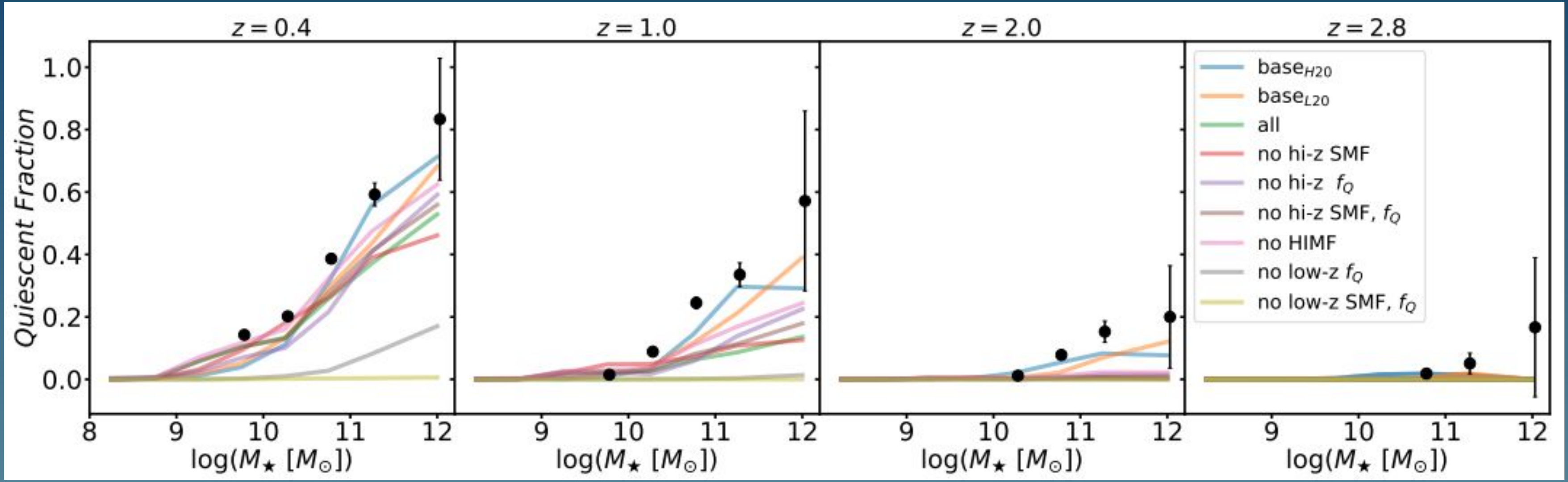

- Reasonably good agreement at z ≲ 1.
- The best models (according to this metric) are those where the number density of SMGs is not used as a constraint
- The low-z f_Q constraint is a key observable.

The Configuration “no HIMF”

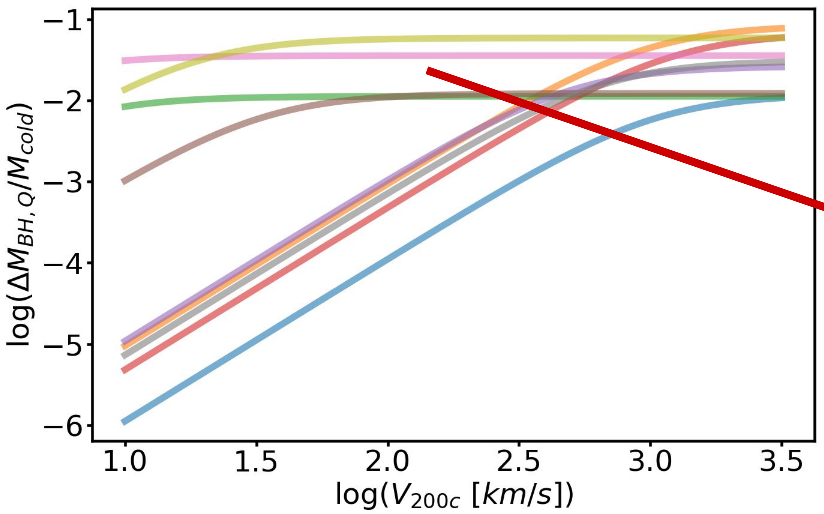

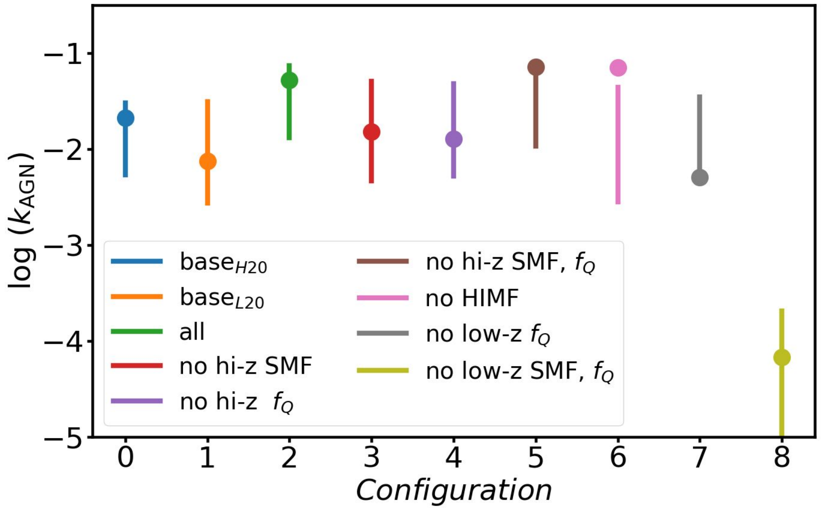

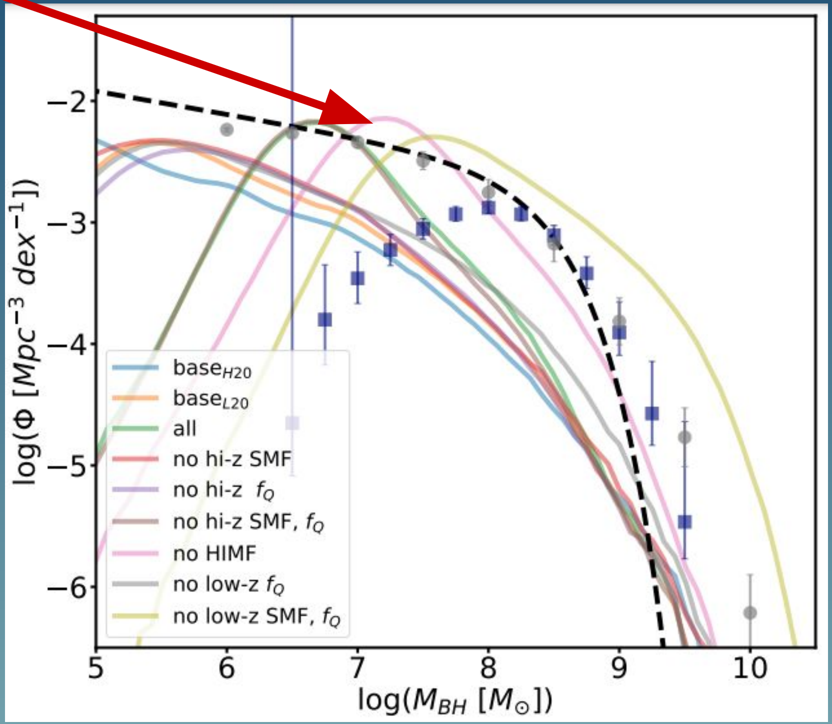

The Main Loss; The Cosmic Star Formation Rate Density

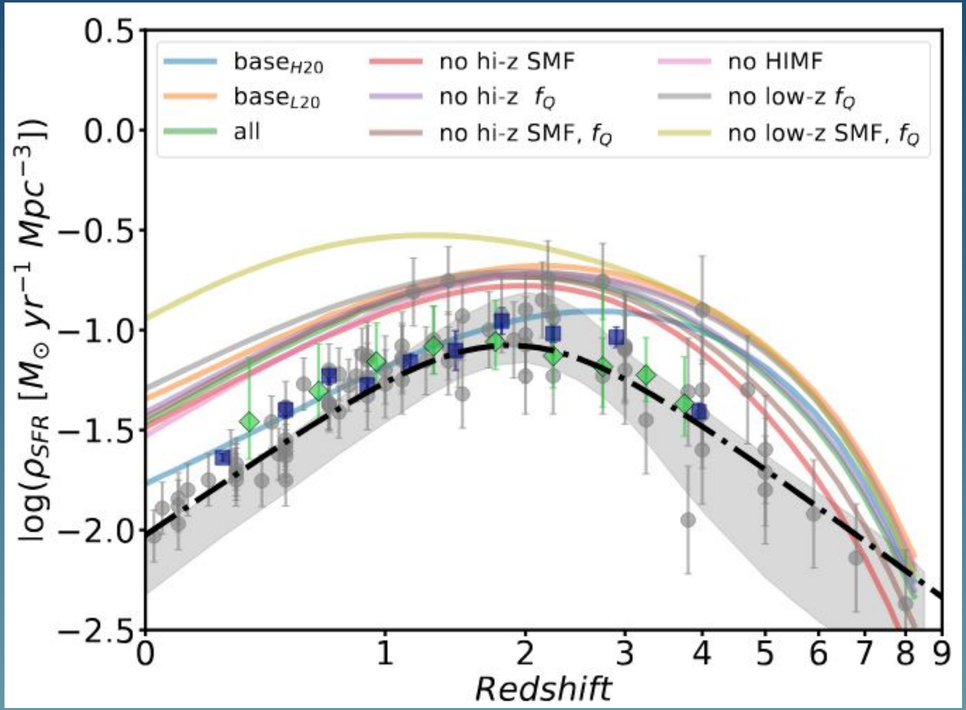

CSFRD is overestimated across most models.

Likely driven by the updated SMFs from Leja+20.